Synthesis and Properties of Ceramic Nanoparticles and Nanocomposites

Dieter Vollath, D. Vinga Szabó and J. Haußelt

Forschungszentrum Karlsruhe, Institut für Materialforschung III, PO Box 3640, D-76021 Karlsruhe, Germany

(Received 8 July 1996; accepted 30 October 1996)

Abstract

This paper describes the possibilities of synthesising ceramic nanoparticles in a microwave plasma. The properties of these particles can be modified by coating them with a layer of a second material. A two-step process to produce this type of particle is described. The structure of these nanocoated particles depends strongly on the crystallisation behaviour of the phases forming the kernel and the coating. The main applications of these new nanocoated particles may either be seen in the formation of diffusion barriers to avoid grain growth or in the modification of physical properties of the core and the chemical properties of the surface. © 1996 Elsevier Science Limited.

1 Introduction

Nanocrystalline ceramic materials or nanoglasses with particle sizes below 10 nm exhibit interesting physical properties.[1] The standard method for synthesis of nanosized oxide powder, the inert gas condensation method developed by Gleiter *et al.*[2,3] and Siegel *et al.*,[4] is a two-step process. In the first step the metal is evaporated and collected as a fine condensate on a cold finger. In a second step the metal condensate is oxidised and then scraped off the cold finger. Nanomaterials can also be synthesised by electron beam evaporation methods[5] or laser ablation.[6] Superfine oxide powders have successfully been produced by flame hydrolysis and hydrothermal synthesis.[7] At the same time and independently Mehta *et al.*[8] and Vollath *et al.*[9–11] developed microwave plasma methods for the synthesis of nanocrystalline ceramic powders. Mehta *et al.*[8] synthesised small amounts of nanocrystalline TiN and TiO_2 at a pressure of 0·7 mbar. Simultaneously a more versatile process using a 915 MHz microwave plasma discharge for the continuous synthesis of oxide or nitride ceramic powders was developed by Vollath *et al.*[9–11] This process uses higher gas pressures in the range from 50 to 100 mbar and a lower frequency, leading to significantly higher production rates.

To show the advantages of the process presented in this paper, it is necessary to explain the physics of a microwave plasma. In an oscillating electric field the energy E transferred to a charged particle is proportional to $\frac{1}{m \times f^2}$, with m = mass and f = frequency. A microwave plasma consists of neutral gas species, dissociated gas and precursor molecules, ions and free electrons. Therefore collisions between charged and uncharged particles influence the energy transfer to the particles. In this case the collision frequency z has to be considered: $E \propto \frac{1}{m} \times \frac{z}{f^2+z^2}$. As the mass of the electrons is small compared to the mass of the ions, a substantial amount of energy is transferred to the electrons at high frequencies, whereas the amount of energy transferred to the ions is small. Thus, the 'temperature' of the free electrons is much higher than the 'temperature' of the ions.[12] Additionally, the temperature of the neutral gas molecules is even lower. This leads to the fact that the 'overall temperature' of a gas passing a microwave plasma is not as high as in a DC or RF plasma, where temperatures in the range from 5000 to 15000°C are obtained. In a microwave plasma the temperature can be adjusted in a range from 300 to 900°C by properly selecting field strength, gas pressure and gas species. Gas pressure and temperature needed for the synthesis of significant amounts of ceramic powders can be adjusted in a range that is optimal for the desired chemical reactions. Additionally, the plasma enhances the kinetics of the chemical reactions by ionisation and the dissociation of the reactive molecules. Therefore, kinetic obstacles can be overcome without increasing the temperature to unacceptably high values. Thus the formation of hard agglomerates in the nanopowders can be avoided. This is one of the main advantages of using a microwave plasma as a means to perform chemical reactions.

In many instances, nanocomposites exhibit mechanical or physical properties of special interest. The main problem in the production of nanocomposites is to obtain a uniform distribution of two or more phases. In general, there are two approaches to produce a uniform nanocomposite:

—Synthesis of a metastable homogeneous mixture and formation of the second phase by precipitation.[13]
—Separate synthesis of the two phases and blending during the step of particle formation.

An excellent uniformity of such a product can be obtained by coating the particles of the first reaction step with the second phase. Sethi and Thölén[14] produced a type of nanocomposite material, consisting of a metal kernel and the corresponding metal oxide as a covering layer by surface oxidation of nanosized metallic powders.

Processes based on mechanical blending do not lead to homogeneous powders on the nanometer scale. Therefore, to obtain the starting material for a uniform nanocomposite of different oxide phases, an approach based on 'nanocoated particles' was selected.[15]

2 The Microwave Plasma Process

Applying the microwave plasma process to the synthesis of oxide or nitride powders, mean particle sizes in the range from 4 to 5 nm are obtained.[11,16,17] Precursor materials to form these nanoscaled ceramic powders are water-free chlorides, carbonyls or metal-organic compounds.

In the case of a chloride precursor, the following reaction may be assumed in the plasma:

(1) Without addition of water:

$$MeCl_n + m/2\ O_2 \rightarrow MeO_m + n/2\ Cl_2$$

(2) With addition of water:

In this case, we have to consider that, besides the dissociation of the water, OH^- radicals are formed in the plasma. Therefore, we have the possibility of two reaction routes:

$$MeCl_n + m/2\ O_2 + n/2\ H_2 \rightarrow MeO_m + n\ HCl$$

and probably

$$MeCl_n + (m + x)OH^- + (m + x)H^+ \rightarrow MeO_m + x\ HClO + (n - x)HCl + (m + 2x - n)H_2$$

where $x << n$ is assumed.

The addition of water has two effects. Through the formation of HCl, and possibly HClO, it increases the reaction enthalpy and acts as a catalyst in increasing dissociation. The temperature of the gas, monitored after passing the reaction (plasma) zone, is generally higher in the case of water addition.

To synthesise nitrides, nitrogen is used as carrier gas. As the chlorides are more stable than the nitrides, it is necessary to add hydrogen to the system. The hydrogen addition enhances the reaction enthalpy and shifts the thermodynamic equilibrium towards the nitrides and HCl. In most cases it is beneficial to use ammonia as hydrogen carrier.

The mechanism of the formation of the nanoparticles is assumed to occur according to the following steps:[17,18]

—Ionisation and dissociation of the reactive components of the plasma.
—Reaction of the dissociated species forming oxide (nitride) molecules.
—Nucleation of the particles by random collision of two or more oxide, respectively nitride molecules.
—Growth of the nuclei by further collision with molecules.
—Further growth by coagulation of the particles.

This process can be extended to produce coated particles.[15] In this context one may think of the synthesis of particles consisting of a core made of an oxide AO_n covered with a second oxide BO_m This goal can be reached by using two identical plasma stages consecutively where each one has its own supply of reactive gases. In the second plasma stage, the processes are identical up to the formation of the molecules of the second oxide BO_m. After the formation of the molecules, the process will be different. As the gas kinetic collision cross-section of the particles formed in the first step is about two orders of magnitude larger than the cross-section of a molecule, the probability of the condensation of B oxide molecules on the A oxide particles is also increased by at least two orders of magnitude. Therefore, one may assume that the particles formed in the first step act as nuclei for the particle formation in the second stage. For detailed quantitative considerations one has to take into account that nucleation energy is necessary for the formation of a new particle. This is not the case if B oxide molecules condense on the surface of the A oxide particles. Therefore, one may expect a high yield in coated particles. Based on these considerations, it is obvious that a small amount of pure particles of B oxide is unavoidable, but it is impossible for any of the A oxide particles to remain uncoated as long as B oxide molecules are present in the second plasma.

3 Experimental Set-Up

In the experimental set-up for the synthesis of ceramic nanopowders, the reaction is performed in a 50 mm diameter reaction vessel made of quartz, passing a TE_{01} mode cavity in sequence connected to a 0·915 GHz microwave generator.[19] The microwave cavity, made of aluminium, is designed as a part of a single-mode microwave system using an IEC 153 R9 (equivalent to RETMA WR 975) waveguide. A maximum of the microwave E-field vector at the centreline of the reaction tube was adjusted using a sliding short and a tri-stub tuner. To obtain nanocoated particles, this experimental set-up was modified by arranging two plasma zones consecutively on one reaction tube. Figure 1 exhibits a schematic view of the arrangement for the synthesis of nanocoated particles. Microwaves, generated in a magnetron, pass an isolator. Then, using an E-plane power splitter, the waveguide is split up into two equal branches. In each of the two branches of the waveguide, the cavities are situated between a tri-stub tuner and a movable short. The E-plane splitter is tuned to obtain a given ratio of the power in both branches. Each of these two branches is equipped with a directional coupler to measure the energy of the forward and backward wave.

To operate two plasma sources, powered by a branched waveguide system, one has to ensure that both plasma sources ignite simultaneously, otherwise it is nearly impossible to ignite the second one. On the other hand, the wave guide settings that are optimal for ignition are usually not the best for plasma operation, which makes the operation of such a branched system difficult. When each branch is optimally adjusted for the maximum field strength at the position of the reaction tube with the tri-stub tuners, a significantly higher strength of the E-field is obtained in the unloaded cavity. This adjustment is best for igniting the plasma. As the burning plasma changes the impedance of the system significantly, the system efficiency obtained with this tuning is not optimal for powder synthesis. For operation, untuned cavities are more advantageous but lead to plasma quenching if operating conditions are changed. This operation mode does not have the best efficiency in the use of the microwaves but it reduces the risk of quenching the plasma. Furthermore, adjusting the power ratio between the two branches, significantly influences the optimal position of the tuners. To avoid this disturbing effect, the two branches of the waveguide are decoupled, using an additional isolator in each branch.

In the experimental realisation of this process, the vapours of the precursors in question are produced outside the reaction chamber and are introduced in front of the plasma reaction zones, respectively. This makes it possible to produce a two-phase composite or nanocoated particles. The temperature of the gas is monitored after passing the reaction (plasma) zones. When water is added, it is important that the water is completely evaporated before it enters the zone where the vaporised precursor is introduced. Otherwise, the droplets act as condensation nuclei for the precursor, leading to very large particle sizes. Also the gas, containing the precursor or the water vapour, has to be hot enough to avoid precipitation. Any precipitation leads to large particle sizes. As a next step, the gas mixture consisting of the carrier gas, the vaporised precursor and, eventually, water vapour, passes the plasma zone where the oxide or nitride nanoparticles are formed.

In a typical run to produce nanocoated oxide particles, a gas volume of about 75 litre min^{-1} STP passes the plasma zone. A mixture of argon with 20 vol% oxygen is used as plasma gas. This gas

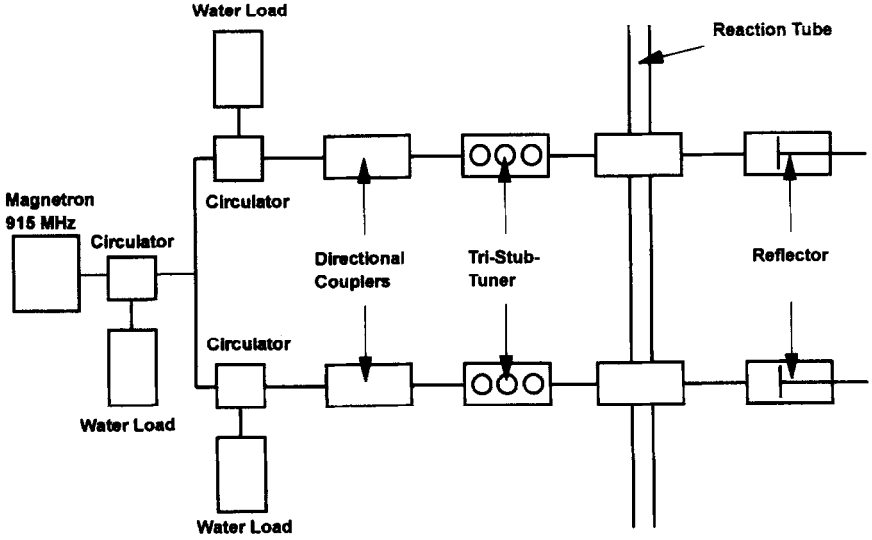

Fig. 1. Experimental set-up for the synthesis of nanocoated particles using a microwave plasma.

carries the evaporated precursor. The pressure in the reaction tube is selected to be within the range from 30 to 50 mbar. The temperature is always kept below 600°C. If possible, an increase of the temperature above 500°C is avoided in order to prevent the formation of hard agglomerates. Keeping the temperature at a low level is difficult, in so far as both plasma sources introduce energy into the system.

The powder is collected on cooled surfaces. The powders are characterised by transmission electron microscopy methods (TEM). Samples from the powders are taken by dipping carbon coated Cu grids into the collected powder.

4 Description of the Products

The production rate and the particle size were found to be correlated. It is possible to produce particles with mean sizes around 8 nm obtaining approximately 1 mol h^{-1} in our experimental equipment. Reducing the mean particle size into the range below 5 nm reduces the production rate significantly. On the other hand the particles with size above 10 nm may be produced at substantially higher rates.

4.1 Single-phase ceramic nanopowders

Single-phase ceramic nanoparticles may be crystalline or glassy. The structure is controlled by the surface energy and the crystallisation energy. Therefore, for each ceramic material a critical particle size controlling the transition glassy–crystalline exists. For alumina, this critical diameter is in the range from 7 to 8 nm.[17] The dark field images reveal a high amount of glassy alumina and show some speckles, indicating crystalline alumina. The electron diffraction patterns exhibit a high amount of diffuse scattering because of the amorphous alumina in the specimen. A minor part of the diffuse scattering may also result from the amorphous carbon film. Finally, in the diffraction patterns there is a faint indication of crystalline alumina particles. The cubic γ-alumina with spinel structure (a = 0·79 nm) fits best to the measured ring spacings and the intensities of the diffraction patterns. High Resolution Electron Microscopy (HREM) reveals that particles with sizes below 7 or 8 nm are amorphous and spherical, whereas larger particles are crystalline and faceted.[17] One- or two-dimensional lattice defects were not found.

In the case of zirconia, the transition from glassy to crystalline should be found with particle sizes below 1 nm. Electron microscopy reveals nearly spherical particles with sizes in the range between 4 and 8 nm. Figure 2 shows a typical bright field electron micrograph of nanocrystalline ZrO_2. As can be seen, the particle size distribution is narrow. Dark field imaging and high resolution electron microscopy show that the individual particles are single crystals. Glassy particles cannot be seen. As expected, dislocations or twins are not found in these small crystals. By electron diffraction the cubic high temperature fluorite structure is identified. This is according to Ostwald's rule that the high-temperature modification is generally formed first. It is assumed that the cubic structure is stabilised by kinetic suppression of the transformation cubic–tetragonal–monoclinic and not by the surface tension introduced by the extremely small particle size.[17] This phenomenon was already observed in the case of zirconia-based ceramic powders synthesised by microwave plasma pyrolysis.[9] In contrast to this the synthesis of ZrO_2 with addition of water leads to a dramatic increase of the particle size: particles with sizes of about 20 to 50 nm are found. The particles are still monocrystals with fluorite structure.

Similar behaviour can be observed in the case of nanocrystalline TiO_2.[17] Independent of the material synthesised, the addition of water leads to significantly larger particle sizes in the range of about 20 nm, compared to about 5 nm obtained without water addition. In both cases the powder particles are single crystals. This is certainly not an effect of the slightly higher reaction temperature. Without water addition, particles of that size were not observed at comparable reaction temperatures. Obviously, water addition can be used as a means of adjusting particle sizes.

The synthesis of Fe_2O_3 results in nearly spherical particles with sizes in the range from 4 to 8 nm for low production rates and in the range from 8 to 12 nm at higher production rates, as shown in Figures 3(a) and (b), respectively. As in the case of zirconia, the particles are single crystals. The cubic

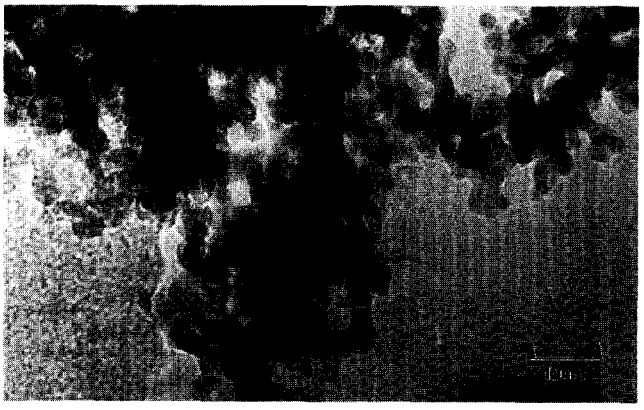

Fig. 2. High resolution electron micrograph of a nanocrystalline ZrO_2 powder. The sizes of the monocrystalline particles are in the range from 4 to 8 nm. Lattice fringes of the cubic ZrO_2 can clearly be seen.

(a)

(b)

Fig. 3. High resolution electron micrograph of nanocrystalline maghemite ex $FeCl_3$: (a) small particles, 4–8 nm, produced at low rates; (b) larger particles, 8–12 nm, produced at higher rates.

γ-Fe_2O_3 with spinel structure (maghemite) was identified by selected area diffraction. Reflections from the α-Fe_2O_3 (hematite) with corundum structure or the tetragonal maghemite, a superlattice structure of the cubic maghemite, are not found in the electron diffraction pattern. From the dark field imaging the presence of small amounts of a glassy Fe_2O_3 phase cannot be excluded.

As was already mentioned, it is also possible to synthesise nitrides. In the simplest case, e.g. ZrN, the product is crystallised in the expected fcc-phase.[16] The mean particle size is in the range from 4 to 8 nm. Figure 4 shows a micrograph of a zirconium nitride powder. Again, the distribution of particle sizes is narrow.

4.2 Nanocoated ceramic particles

Nanocoated ceramic particles can be obtained only if the phase diagram exhibits neither a mutual solubility nor a compound consisting of the two phases. This is a fundamental condition for the synthesis of coated nanoparticles. Depending on the crystallisation behaviour of the two phases

Fig. 4. Bright field image of nanocrystalline ZrN powder.

forming core and coating, two different types of nanocoated particles are observed. The typical structures observed in these cases are explained on the basis of the system Al_2O_3–ZrO_2. This system was chosen as a model nanocomposite material because alumina and zirconia exhibit a very low mutual solubility and do not form any compound.[20]

The first type is characterised by the existence of at least one glassy phase. Independent of the particle size, zirconia is always found to crystallise in the cubic structure. Alumina particles smaller than about 8 nm are amorphous. Therefore, combinations of these two oxides are perfect examples of this type of nanocomposite. One of the structures to be explained in this case is depicted in Fig. 5. The particles shown in this micrograph consist of a core of zirconia surrounded by a coating of alumina. The core is crystalline, whereas the coating is amorphous. Two of the cores were in an orientation for lattice imaging, whereas the third particle did not have a proper orientation to obtain lattice fringes. The sizes of the cores range from 4 to 6 nm. The thickness of the amorphous coating is in the range from 1 to 2 nm.

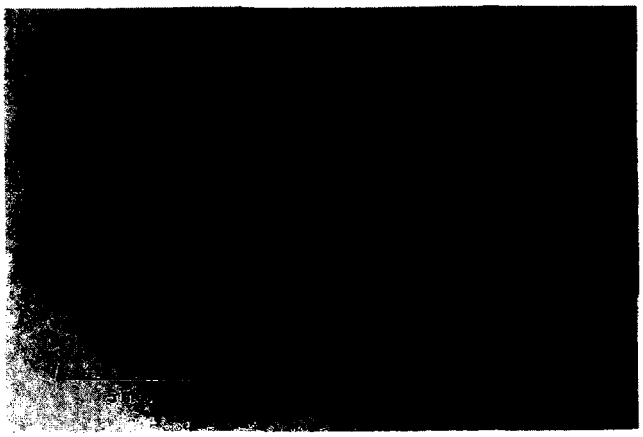

Fig. 5. Zirconia particles coated with alumina. The striations within the core (lattice fringes) represent an image of the zirconia {111} lattice planes with spacings of 0·29 nm. The alumina coating is glassy.

In the inverse case shown in Fig. 6, where the core consists of glassy alumina and the coating of crystallised zirconia, electron microscopy shows primarily the lattice fringes of the zirconia coating. The centre of these particles is brighter than their outer regions. This is because of the weaker absorption of the electrons in the amorphous alumina kernel as compared with the zirconia coating. Furthermore, the lattice image of the zirconia changes only in contrast but not in the image itself, indicating a change in thickness but not in crystal structure.

The second case is characterised by the fact that both phases are crystallised. In this case spherical particles with diameters from 6 to 10 nm are found. They have a crystalline core of zirconia with a diameter of about 2 – 3 nm, as well as a crystalline γ-alumina coating with a thickness of about 2–3 nm. Figure 7 demonstrates the appearance of such a particle consisting of a small zirconia kernel coated with crystallised alumina.

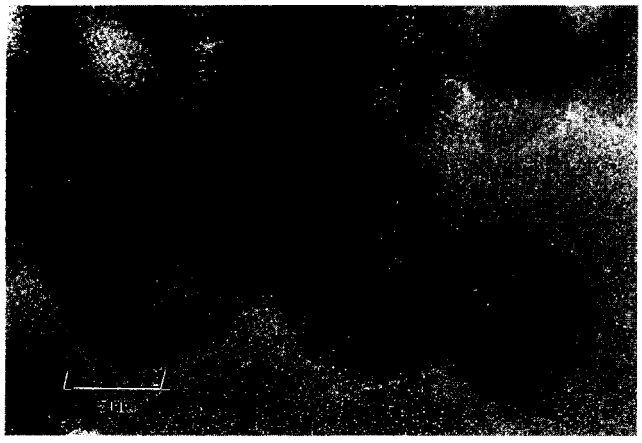

Fig. 6. Glassy alumina particles coated with crystallised zirconia. The alumina cores cause the brighter centre of the particles in the micrograph.

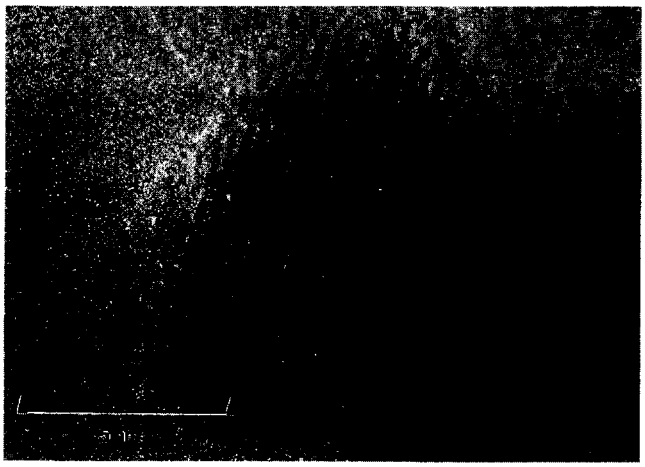

Fig. 7. Crystallised zirconia particle coated with crystallised alumina. The lattice fringes in this micrograph, representing the structure of the coating, may be interpreted as {211} fringes of the γ-alumina coating. As is indicated by arrows, the coating contains dislocation-like structures. Three additional half planes with opposite directions are inserted.

The lattice fringes with spacings of 0·32 nm in this micrograph represent the structure of the coating. They may be interpreted as {211} fringes of the γ-alumina coating grown epitactically on the {111} or {110} plane of the zirconia core. The topotactic misfit[21] in this case is about 10%. A misfit of that amount needs dislocations for the adjustment of the two structures. Detailed analysis of the lattice fringes in the micrographs reveals that the coating of this type of particle contains dislocation-like structures as lattice defects. There are three additional {211} half planes inserted, having opposite directions. An arrangement of dislocations like this should annihilate. As these dislocations are not annihilated, one may assume that these dislocations are sessile and necessary to compensate the lattice misfit. This is in good agreement with the general opinion that it is impossible to maintain mobile dislocations in nanoparticles.

Additionally, point analyses of coated ZrO_2/Al_2O_3 particles were performed by energy dispersive X-ray microanalysis in a dedicated STEM.[22] It was shown that the cation ratios Zr/Al of the cores are significantly higher than the cation ratios Zr/Al of the coatings. Since the particles are completely coated, X-ray signals from the coating cannot be avoided while acquiring the spectra from the cores. Additionally, these results are influenced by the specimen drift and contamination as well as by beam damage during spectrum acquisition.

5 Application of Nanocoated Particles

Coated nanoparticles are an entirely new class of materials, with a high potential for new applications. The combination of two materials on a nanometer scale, one acting as core and the other as coating, will result in interesting physical and chemical properties and thus will result in new applications. With an increasing number of different types of nanocoated particle and an increasing understanding of the resulting physical and chemical properties due to the small particles embedded in a second phase, new, interesting applications should become available. Three potential, rather 'conventional' application fields are described in this section. New applications based on quantum confinement phenomena are, for the moment, excluded.

5.1 Diffusion barrier to avoid grain growth in nanomaterials

As it is a necessary prerequisite for the synthesis of nanocoated particles that the mutual solubility

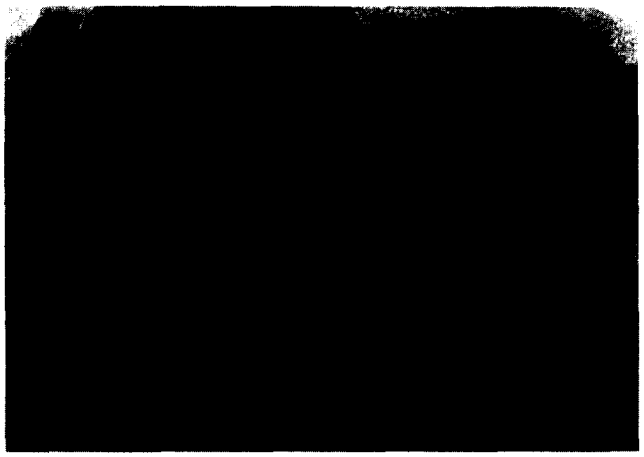

Fig. 8. Sintered zirconia–alumina nanocomposite. The zirconia particles remain separated by the surrounding alumina.

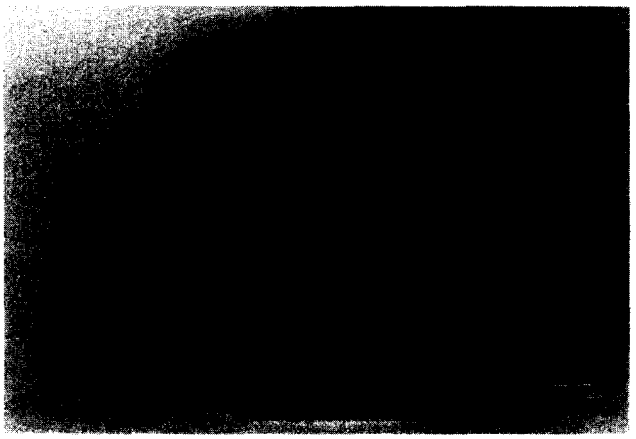

Fig. 9. Crystallised maghemite (γ-Fe_2O_3) particle coated with crystallised zirconia. The particle is characterised by the lattice fringes of the cubic zirconia {111} planes and a brighter centre without lattice fringes.

is close to nil, it is obvious that the coating acts as a diffusion barrier. Such a diffusion barrier thwarts grain growth until that moment where the coating material forms grains. Usually it is possible to get sufficient sintering before the kernels come into direct contact. Figure 8 depicts this situation for a sintered specimen. This specimen was made of a powder consisting of zirconia coated with alumina. In this figure, one can clearly see that the material is already compacted, but the zirconia particles are still separated. This behaviour is essential when physical properties depend strongly on the size of the particles.

5.2 Modification of the physical properties

An example of an important, strongly grain-size-dependent property is magnetism. Ferrimagnetic particles of maghemite (γ-Fe_2O_3) with sizes in the range up to about 8 nm are superparamagnetic.[23] During sintering of such a powder two detrimental processes may occur:

—The material loses its superparamagnetism because of the grain growth.
—The magnetic particles start forming larger magnetic clusters, which are no longer superparamagnetic.

The impact of these processes on superparamagnetism can be reduced by coating the magnetic particles with a layer of a second oxide. To prove this, nanocoated particles in the system maghemite–zirconia were produced. The particles consist of a maghemite core that is coated with zirconia. Figure 9 shows a typical example for a maghemite particle with a diameter of about 8 nm coated with zirconia. In total this particle has a diameter of about 15 nm. The micrograph of the particle is characterised by the lattice fringes of the cubic zirconia. The contrast between core and coating is less pronounced than in the case of the system discussed in the previous chapter because the difference in atomic number between iron and zirconium is significantly smaller than in the case of aluminium and zirconium. To demonstrate the influence on the magnetic properties, the magnetisation curves for uncoated and coated maghemite[24] are shown in Fig. 10. Although the coated particles contain less iron oxide than the uncoated ones, the magnetisation increases with the coating. This change in the properties can also be seen in the Mößbauer spectrum.[24]

5.3 Modification of the chemical surface properties

Nanoparticles are used as carriers for active organic ligands for many applications in medicine and pharmacology.[25,26] It is sometimes difficult to attach such ligands on the surface of a nanoparticle. In this case it is of great importance to modify the particle surface by coating with a material better suited for the attachment of a specific organic compound.

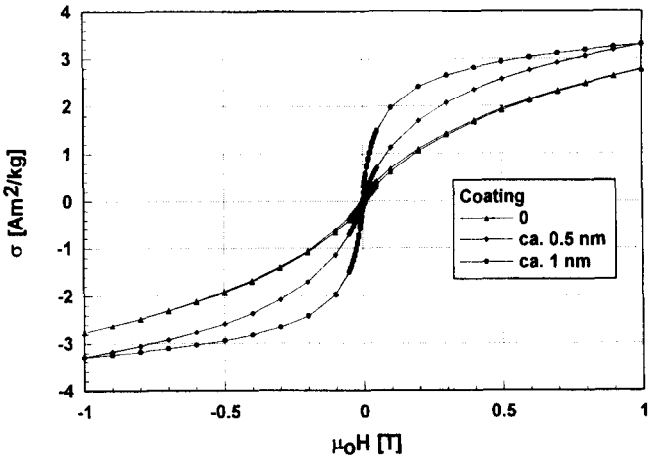

Fig. 10. Magnetisation curve of uncoated and zirconia coated maghemite (γ-Fe_2O_3) particles.

6 Conclusions

Microwave plasma synthesis is well suited to obtain nanoparticulate ceramic powders. Because of the specific conditions during synthesis, the reaction product does not form hard agglomerates. Additionally, it has been demonstrated that it is possible to prepare ceramic particles with sizes below 10 nm consisting of two different oxides in the core and the coating by using a two-step microwave plasma process. The structure of these particles depends strongly on the crystallisation behaviour of the phases for the kernel and the coating. The main advantages of these new nanocoated particles may be seen in the formation of diffusion barriers and in the modification of the physical and chemical properties of the surface.

References

1. Gleiter, H. Nanocrystalline materials. *Prog. Mater. Science*, 1989, **33**, 223–315.
2. Karch, J., Birringer, R. and Gleiter, H. Ceramics ductile at low temperature. *Nature*, 1987, **330**, 556–558.
3. Gleiter, H. Materials with ultrafine microstructures: retrospectives and perspectives. *Nanostructured Materials*, 1992, **1**, 1–19.
4. Hahn, H., Eastman, J. A. and Siegel, R. W. Processing of nanophase ceramics. *Ceram. Trans.*, 1988, **B1**, 1115–1122.
5. Günther, B. and Kumpmann, A. Ultrafine oxide powders prepared by inert gas evaporation. *Nanostructured Materials*, 1992, **1**, 27–30.
6. LaiHing, K., Cheng, P. Y. and Ducan, M. A. Ultraviolet photolysis in a laser vaporization cluster source: synthesis of novel mixed-metal clusters. *J. Phys. Chem.*, 1987, **91**, 6521–6525.
7. Kriechbaum, G. W. and Kleinschmit, P. Superfine oxide powders—flame hydrolysis and hydrothermal synthesis. *Angew. Chem. Adv. Mater.*, 1989, **101**, 1446–1453.
8. Mehta, P., Singh, A. K. and Kingon, A. I. Nonthermal microwave plasma synthesis of crystalline titanium oxide and titanium nitride nanoparticles. In *Mater. Res. Soc. Symp. Proc.*, 1992, **249**, 153–158.
9. Vollath, D., Sickafus, K. and Varma, R. Synthesis of nanocrystalline powders for oxide ceramics by microwave plasma pyrolysis. In *Mater. Res. Soc. Symp. Proc.*, 1992, **269**, 379–384.
10. Vollath, D. and Sickafus, K. E. Synthesis of nanosized ceramic oxide powders by microwave plasma reactions. *Nanostructured Materials*, 1992, **1**, 427–437.
11. Vollath, D. and Sickafus, K. E. Synthesis of ceramic oxide powders in a microwave plasma device. *J. Mater. Res.*, 1993, **8**, 2978–2984.
12. McDonald, A. D., *Microwave Breakdown in Gases*. John Wiley & Sons, New York 1966.
13. Vollath, D. and Szabó, D. V., Synthesis of ceramic nanocomposites in a microwave plasma. In *Proceedings of CIMTEC 8*, Florence, 1994, in press.
14. Sethi, S. A. and Thölén, A. R., A TEM study of oxides formed on ultrafine Fe, Cr and Fe–Cr particles. *Nanostructured Materials*, 1993, **2**, 615–622.
15. Vollath, D. and Szabó, D. V., Nanocoated particles: a special type of ceramic powder. *Nanostructured Materials*, 1994, **4**, 927–938.
16. Vollath, D. and Sickafus, K. E., Synthesis of nanosized ceramic nitride powders by microwave supported plasma reactions. *Nanostructured Materials*, 1993, **2**, 451–456.
17. Vollath, D., Synthesis of nanocrystalline ceramic powders in a microwave plasma (in German). *KfK-Nachrichten*, 1993, **25**, 139–144.
18. Vollath, D. and Sickafus, K. E., A continuous process to produce nanophased ceramic powders. In *Proceedings of Third Euro-Ceramics*, Vol. 1, 1994, 9–14.
19. Vollath, D., A cascaded microwave plasma source for synthesis of ceramic nanocomposite powders. In *Mater. Res. Soc. Symp. Proc.*, 1994, **347**, 629–634.
20. The American Ceramic Society, *Phase Diagrams for Ceramists*. Westerville, OH, USA, 1975, p. 135.
21. Matthews, J. W., Misfit Dislocations. In *Misfit Dislocations in Solids*, ed. F. R. N. Nabarro. North Holland, Amsterdam, 1979.
22. Szabó, D. V. and Müllejans, H., Characterization of nanocomposites by electron microscopy methods. In *Proceedings of the ICEM 13*, Vol. 2B. Les Éditions de Physique, Paris, 1994, pp. 379–380.
23. Vollath, D., Szabó, D. V., Taylor R. D., Willis J. O. and Sickafus K. E., Synthesis and properties of nanocrystalline superparamagnetic γ-Fe_2O_3. *Nanostructured Materials*, 1995, **6**, 941–944.
24. Vollath, D. and Szabó, D. V., Synthesis and properties of coated nanoparticles. In *Proceedings of the Gorham Conference on Nanostructured Materials and Coatings '95*, Atlanta, USA.
25. Pfefferer, D., Wagner, S., Kresse, M., Taupitz, M. and Ebert, W., MR-aniography with superparamagnetic iron oxide particles: optimisation of particle size and physicochemical properties. *ECR '95*, Vienna, Austria, 5–10 March 1995.
26. Jordan, A., Wust, P., Fähling, H., Jahn, W., Hinz, A. and Felix, R., Inductive heating of ferrimagnetic particles and magnetic fluids: physical evaluation of their potential for hyperthermia. *Int. J. Hyperthermia*, 1993, **9**, 51–68.